11th SAGA Biennial Technical Meeting and Exhibition
Swaziland, 16 - 18 September 2009, pages 588 - 593

Assessing the degree of synchronization between geophysical records using the method of instantaneous phase differences

O. J. Botai[1], W. L. Combrinck[1, 2], V. Sivakumar[1, 3]

1. Department of Geography, Geoinformatics and Meteorology, University of Pretoria, South Africa, joel.botai@up.ac.za
2. Space Geodesy, Hartebeestshoek Radio Astronomy Observatory, South Africa, ludwig@hartrao.ac.za
3. National laser center, Council for scientific and industrial research, South Africa, svkumar@csir.ac.za

ABSTRACT

Recovering geodetic parameters such as tropospheric delay and geodetic site positions and monitoring their variations in time has important applications for studying the processes of the dynamic Earth. Geodetic position time series exhibit non-linear motions that are associated with seasonal signals caused by loading effects, and seismic deformation processes such as earthquakes etc. This implies that the fluctuations in the station coordinates and tropospheric parameters could be synchronized because they are driven by common underlying processes. In the analysis of space geodetic measurements, space geodetic solutions are often co-assessed in order to determine geophysical signals present in both parameters. The main objective presented in the current contribution is to determine the linkage between temporal structure of the zenith tropospheric delay and the geodetic station height coordinates fluctuations in the time-frequency-energy space. The temporal structures of the combined solution of the zenith tropospheric wet delay (ZWD) and the geodetic station height at the Hartebeesthoek geodetic station (HartRAO) have been studied. The oscillation patterns in these geophysical signals have been analysed by using the noise-assisted data analysis (NADA) methodology known as ensemble empirical mode decomposition (EEMD). The instantaneous phase differences among the associated modes of the intrinsic mode functions (IMFs) have been computed and used to assess the degree of synchronisation between the two series. Our results show that the ZWD and the HartRAO geodetic station height show modes that are temporally correlated and some of the IMF modes exhibit temporal structures that can be associated with both local and global forcing mechanisms.

Keywords: Geodetic parameters, ZWD, EEMD, correlation, phase differences

INTRODUCTION

The use of geodetic observations to study processes that shape the Earth system science finds justification in the kind of information about the dynamic Earth inherent in geophysical signals embedded in the geodetic data. For instance, deformation of the surface of Earth has been detected in Global Navigation Satellite System (GNSS) data (e.g., Dong *et al*., 2002) and in Very Long Baseline Interferometry (VLBI) analysis (e.g., van Dam and Herring, 1994; Petrov and Boy, 2004). Due to various aspects such as nonlinear motions of the Earth and atmosphere and the systematic differences in the observations, geodetic data records exhibit nonlinear and nonstationary properties. In addition, the solution of the datum and atmospheric parameters and site positions derived from various space geodetic techniques such GNSS, VLBI, Satellite Laser Ranging (SLR), Doppler Orbitography and Radiopositioning Integrated by Satellite (DORIS) are influenced by 1) the type of geodetic technique, 2) geodetic analysis strategy and solution related problems and 3) real geophysical signals. Inter-technique analysis strategy is often used to remove technique dependent and systematic biases. Additionally, analyses of geodetic observations from co-located techniques are also used to identify discrepancies between techniques and optimise the different strengths of each technique (Krugel *et al*., 2007).

Geodetic position time series show evidence of nonlinear motions that are associated with signals of varying time scales caused by e.g. loading effects, and seismic deformation processes such as earthquakes. Mendes et al., (2005) investigated station coordinates and baseline lengths of some Asian geodetic site time series and recovered up to 9 mm amplitudes of seasonal components in the height components. Additionally, Dodson *et al*., (1995) analysed and found a significant correlation (0.91) between the variability of the wet delay measured using the water vapour radiometer (WVR) at Onsala site and the absolute value of the

residual error in the height based on a 134 km baseline from Onsala to Jonkoping. The results reported in Dodson *et al*., (1995) suggests that atmospheric variability as inferred from space geodetic data includes information of the accuracy of the geodetic site positions. This implies that the fluctuations in the station coordinates and tropospheric parameters could be synchronised because they are driven by common underlying processes. In the analysis of space geodetic measurements, space geodetic solutions are often co-assessed in order to determine and characterise the nature of the underlying geophysical signals manifested in the variability of the geodetic parameters (Krügel *et al*., 2007).

In this contribution, the noise-assisted data analysis (NADA) methodology called the Ensemble Empirical Mode Decomposition (EEMD) described in Zhaohua and Huang, (2009) is used to extract the intrinsic properties of the combined solution of geodetic tropospheric ZWD and geodetic station height measured at HartRAO - South Africa over six years between 2000 and 2005. The methodology used to compute the combined solution of the ZWD derived from VLBI observations is described in Heinkelmann *et al*., (2007). The EEMD is an improvement to the Empirical Mode Decomposition (EMD) and Hilbert-Huang Transform methodology described in Huang *et al*., (1998). In the present paper, we only focus on assessing degree of synchronization by use of phase differences of the instantaneous frequencies of the IMFs of the tropospheric ZWD and geodetic station coordinates. The correlation strategy employed here involves the linkage of instantaneous phase differences among the associated ZWD and geodetic height IMF modes derived from the EEMD with a set threshold value. In particular, the amplitude level of the first IMF mode is taken as the reference amplitude of the noisy IMFs in the data.

The EMD and HHT is a new cutting-edge methodology that is widely used in many scientific fields such as natural (Salisbury and Wimbush, 2002, Shen et *al.*, 2005) and engineering (Huang *et al*., 2005) sciences. For instance, Salisbury and Wimbush (2002), used Southern Oscillation Index (SOI) data and applied the HHT technique to determine whether the SOI data are sufficiently noise free that useful predictions can be made and whether future El Nino southern oscillation (ENSO) events can be predicted from SOI. Based on annual and seasonal averages of temperature, cloudiness, air pressure, and global radiation and precipitation measurements at Zagreb-Grič over the period 1862-2002, Radić et al, (2004) used EMD to study the climatic fluctuations over the north-west part of Croatia and reported of the presence of climatic fluctuations on decade-to-century scales in the sums of the low IMFs. More recently, Pegram *et al*., (2008) suggested an improvement to the original EMD algorithm using rational splines and the flexible treatment of the end conditions and applied it to the rainfall time series.

In the application of the HHT to tropospheric zenith wet delay and geodetic station analysis, the intrinsic mode functions and their Hilbert transform can be used to: 1) represent the frequency/wavelength content of the parameters; 2) filter the data in the temporal domain in preparation for secondary analyses such as correlation analyses of ZWD and geodetic station height, and 3) compare ZWD derived from different geodetic techniques and assess their similarities by performing simultaneous temporal analyses. In addition, the goal of the analysis would be to isolate and extract meaningful geophysical signals in the data so as to aid in describing the underlying physics/phenomena of the tropospheric data.

METHOD AND RESULTS

The geodetic data under consideration is often measured at different spatial-temporal scales. The geodetic record analysed in the present contribution were based on data measurements covering a period of six years between 2000 and 2005. The ZWD and geodetic height considered in the analysis are plotted in Figure 1. The plotted ZWD and local coordinate system (East-North-Up: ENU) have a mean of zero. The local ENU coordinates were transformed to the geodetic longitude, latitude and height. The geodetic height coordinate is considered here because it is the most sensitive component to some physical processes such as loading of the crust by the atmosphere, oceans and surface water (Dong et al., 2002; Trogoning and van Dam, 2005).

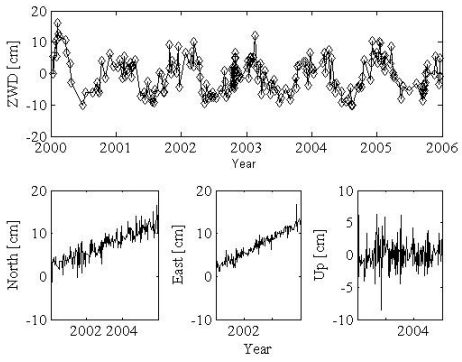

Figure 1. ZWD and local coordinate (NEU) system at HartRAO.

The EEMD methodology used in the present analysis, finite, non-infinitesimal ratio of the standard deviation of the added noise and that of ensemble of 35% is used to force the ensemble data to exhaust all possible solutions in the sifting process, thus requiring the different scale signals to collate in the proper intrinsic mode functions (IMF) dictated by the dyadic filter banks (Zhaohua and Huang, 2009). The effect of the added white noise is to present a uniform reference

frame in the time-frequency and time-scale space. This implies that the added noise provides a natural reference for the signals of comparable scale to collate in one IMF. With this ensemble mean, the scale can be clearly and naturally separated without any a priori subjective criterion selection, such as in the intermittence test for the original EMD algorithm. This new approach fully utilizes the statistical characteristics of white noise to perturb the data in its true solution neighbourhood, and then cancel itself out through the ensemble averaging (Zhaohua and Huang, 2009).

Herein, the i^{th} geodetic data time series (ZWD and geodetic height) can be modelled by equation (1);

$$Y_i^t = Y^t + \varepsilon_i^t \qquad (1)$$

In equation (1), the ε_i^t is white noise external component that decreases the signal-to-noise ratio in the geodetic ZWD and station height series. This external component serves to provide the uniform reference scale useful for signal extraction from the data during EEMD. In general, the EEMD algorithm can be stated as follows:

1. add white noise to the data (Y_i^t),
2. decompose the data with added ω_i^t into the IMFs,
3. repeat (1) and (2) several times each time adding different ω_i^t ,
4. as a final result, obtain the means of the corresponding decomposed IMFs.

As stated earlier, the amplitude level of IMF_1 is taken as the reference amplitude of the noisy IMFs in the data. The assumption taken here is that, the first IMF (with highest frequency) is corrupted with noise. Therefore the criterion of selecting meaning empirical IMFs is based on the proportion of the amplitude of target IMF to the reference amplitude. Herein, the amplitude of the selected amplitude ought to be about 25% of the maximum amplitude of the reference IMF. The rationale behind this criterion is derived from the relationship between amplitude of the IMF and the total energy of the IMF: the square of the amplitude is the equivalent to the energy of the IMF. As a result, the criterion used here utilizes only significant oscillating IMFs.

The phase differences between the selected IMF derived from ZWD and geodetic height are calculated in order to evaluate the degree of linkage between the different modes of the respective IMFs. Using the Hilbert transform, the local frequencies of each IMF mode can be computed using the method described in Huang, *et al*., (1998) and further re-defined in Zhaohua and Huang, (2009). In this work, we concentrate on the projection of the phase shift defined by equation (2);

$$\varpi_{i,j}^t = \square\, e\left(e^{i\Delta\theta_{i,j}^t}\right) \qquad (2)$$

where $\Delta\theta_{i,j}^t = \left|\theta_i^t - \theta_j^t\right|$. In order to determine the closeness of the modes, a global indicator of the constant phase shift between ZWD and geodetic height; the variance of $\varpi(:)$ is computed. The constraint used to detect pairs of modes with constant phase shift in this contribution is that of $\mathrm{var}\left[\varpi(:)\right] \le 0.33$. In this case, IMFs with $\mathrm{var}\left[\varpi(:)\right] \ge 0.33$ have different local frequencies and therefore have weak or no correlation.

The computed ZWD and geodetic station height IMFs are plotted in

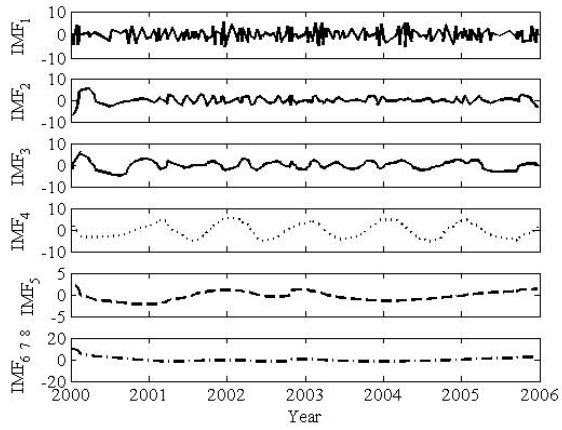

Figure 2 and

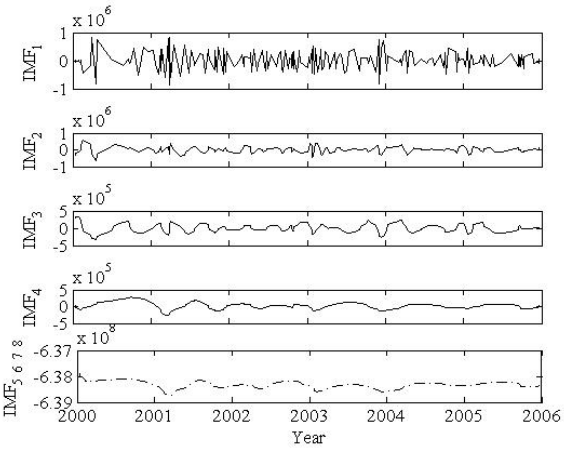

Figure 3 respectively. The original IMFs (from short to long periods) are plotted from top to bottom. During the decomposition stage, eight IMFs were derived. The decomposition of ZWD and geodetic station height separated modes from those with local high frequencies to ones with low local frequencies. $IMF_{6,7,8}$ derived

from the ZWD in

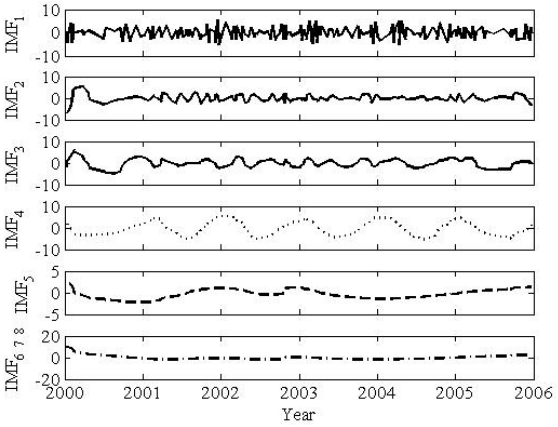

Figure 2 were combined in order to determine the nonlinear trend in the data. $IMF_{1\&2}$ are the most highly fluctuating modes and could be associated to processes with fluctuations corresponding to diurnal to monthly time scales and are mostly sensitive to the noise. Processes such as local weather systems e.g., the passage of cold fronts and wind are likely to cause this fluctuating mode. In addition, seasonal fluctuations dominate IMF_3. This mode could be representative of the regional circulation systems such as the ITCZ. IMF_4 depicts a clear annual signature. This mode could be driven by processes that are global such as the ENSO.

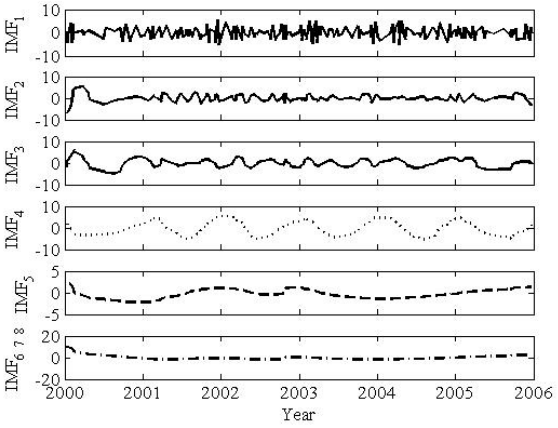

Figure 2. IMFs computed from combined ZWD. The bottom panel represents the nonlinear trend component in ZWD

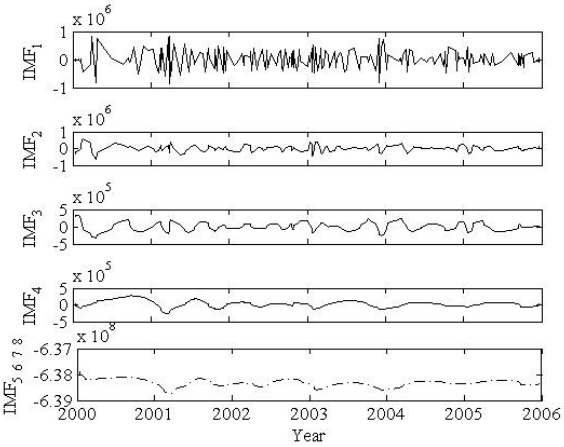

Figure 3. IMFs derived from geodetic station height.

The observed low frequency IMFs in

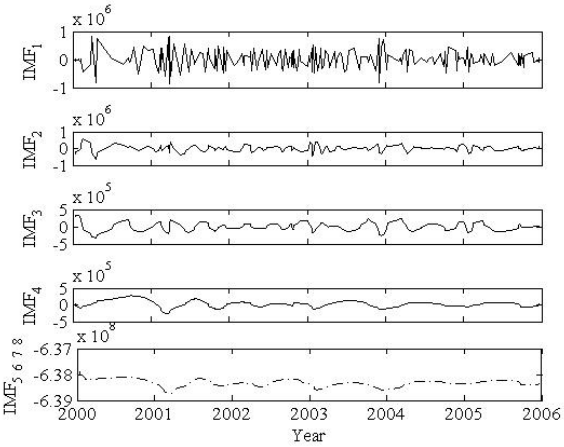

Figure 3 could be associated to the fluctuations that are driven by common underlying physical processes, while the high-frequency IMFs could be attributed to noise in the data and to external forcings. As depicted in

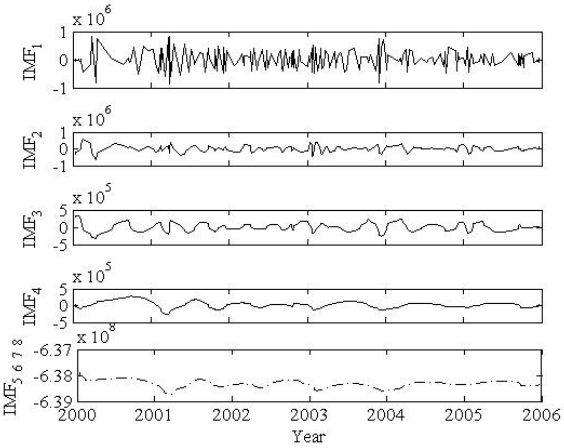

Figure 3 , the local periods are not constant but for each fixed IMFs, they are constrained within different ranges. Overall, the modes of oscillation in the geodetic station height show highly

frequency oscillations. The geodetic height IMFs plotted in

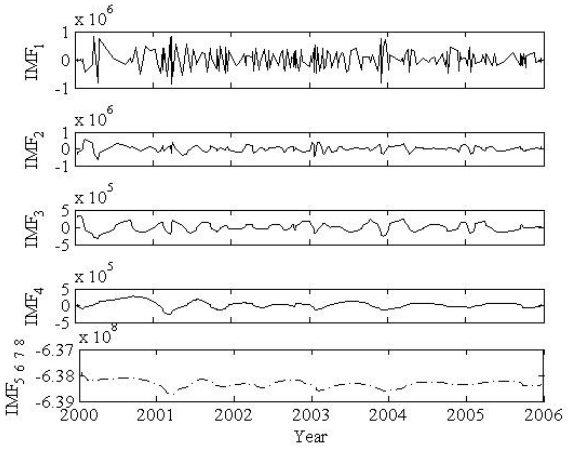

Figure 3 exhibit oscillation patterns with characteristic periods; annual (IMF_4 mode), seasonal (IMF_3 mode), monthly (IMF_2 mode) and diurnal ($IMF_{<2}$ mode) components. $IMF_{6, 7, 8}$ corresponds to the nonlinear trend which exhibits both fluctuating decreasing trend.

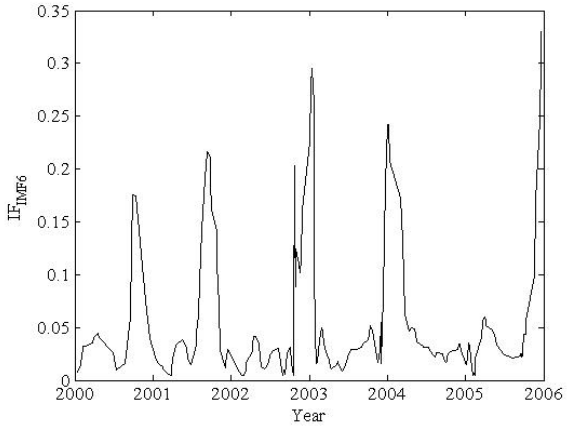

Figure 4. Instantaneous frequency corresponding of the selected ZWD IMFs.

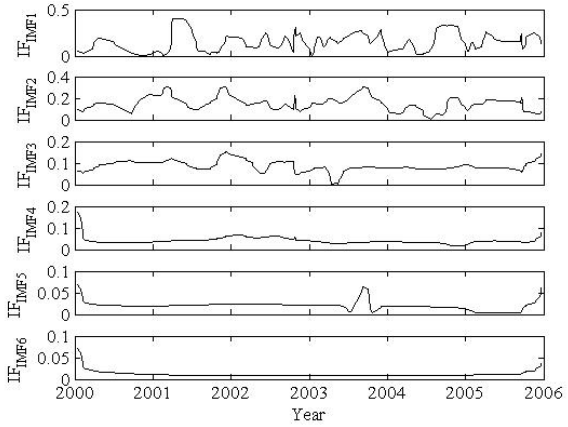

Figure 5. Instantaneous frequencies corresponding to the selected geodetic height IMFs.

Since not all the IMFs extracted from ZWD and geodetic heights are physically significant, the criteria outlined earlier was used to select instantaneous frequencies for computing the phase shifts. Based on the set threshold of 0.33, instantaneous frequencies corresponding to IMF_6 and $IMF_{1, 2, 3, 4, 5, 6}$ modes from ZWD and geodetic height respectively were considered for calculating the phase shift. Figure 4 and Figure 5 depicts the local frequencies of the IMFs selected and used to derive the variance matrix that is used to evaluate the degree of synchronization between ZWD and geodetic height fluctuations. As can be observed, only the instantaneous frequencies (unit: cycles per fraction of a year) of the IMF_6 mode of the ZWD was selected. As illustrated in Figure 4, the instantaneous frequency is dominated by an inter-annual and annual temporal structure. The amplitude of this frequency tends to the maximum during summer months. This behaviour could be attributed to high moisture flux density experienced by the Highveld climatic conditions of South Africa during summer months. The amplitudes of the instantaneous frequencies of the $IMF_{1, 2, 3, 4, 5, 6}$ corresponding to the geodetic height vary between 0.1 and 0.5. The instantaneous frequencies of $IMF_{1, 2, 3}$ modes show seasonal and inter-annual variability while the frequencies for $IMF_{4\&5}$ modes show annual signature. This implies that the IMFs modes derived from geodetic station height characterise the seasonal, inter-annual and annual periodicity of the underlying processes. From the variance matrix, six pairs of modes of IMFs were considered to be exhibit lasting periods of synchronization with fluctuating phase coincidence as depicted in

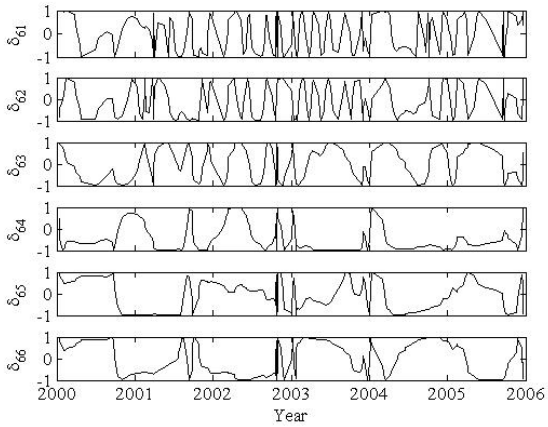

Figure 6.

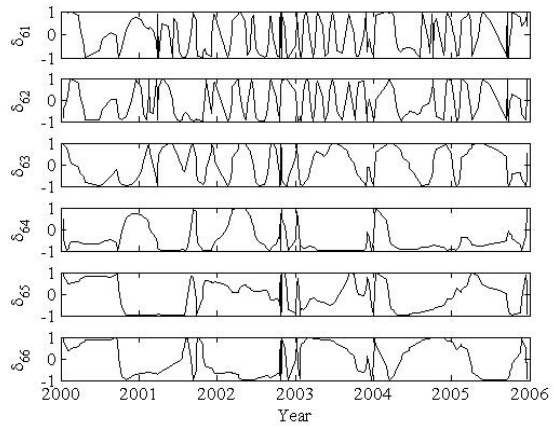

Figure 6. Phase shift of ZWD and geodetic station height of the selected IMFs modes.

It can be observed that, in most of the IMFs couples selected with synchronization, the phase coincidence fluctuates between 1 and -1 over the entire time period of the data. The correlations by pairs indicate that the common fluctuations in ZWD and mean geodetic height could be associated to both local and non-local processes. The decreasing temporal dependence of phase coincidence between ZWD and geodetic station height is inferred from the current analysis. This unique feature has strong seasonal signature at δ_{61} and low oscillations at δ_{66}. As a result, local high frequency oscillations from local underlying processes could be responsible for driving these fluctuations. These processes are related to local weather conditions such as heat waves and cold fronts which are common in the Highveld climatic region. The temporal dependence of phase shift seems to suggest that the ZWD and geodetic height fluctuations are strongly nonlinear with oscillating structures that are visible in the phase shifts. The nonlinear fluctuations could have been triggered possibly by various stochastic resonance phenomena such as the inter-tropical convergence zone (ITCZ), ENSO and other trade winds.

CONCLUSIONS

Atmospheric variability signature as inferred from space geodetic data includes information on geodetic site positions. The high linear correlation of ZWD and geodetic station height reported in the literature (e.g., Dodson *et al*., 1995; Mendes and Langley, 1998; Yin *et al*., 2008; Wang *et al*., 2008) assumed that the underlying processes responsible for the spatial-temporal variability of ZWD and geodetic site positions are linear and stationary. In the present contribution, this assumption is not upheld, rather, the method of phase differences of the EEMD IMFs is used to determine periods of phase coincidence. The advantage of using EEMD is that it adaptively decomposes the ZWD and geodetic fluctuations into different scales based on the local characteristic time scale of the data. In the current analysis, it is found that the fluctuations of ZWD over HartRAO and the geodetic station height have a time dependent phase coincident and therefore are driven by strongly nonlinear stochastic processes that are local and non-local forces that are triggered by stochastic resonance-like process.

ACKNOWLEDGMENTS

This research is partly supported by Inkaba yeAfrica project, a German-South African collaborative Earth Sciences initiative. The authors would like to express their gratitude to Dipl.-Ing. Dr. Robert Heinkelmann of the Deutsches Geodätisches Forschungsinstitut (DGFI) for providing data.

REFERENCES

Dong, D., Fang P., Bock Y., Cheng M. K., and Miyazaki S., (2002), Anatomy of apparent seasonal variations from GPS-derived site position time series, Journal of Geophysical Research., 107(B4), 2075, doi:10.1029/2001JB000573.

Dodson A. H., Shardlow P. J., Hubbard L. C. M., Elgered G., and Jarlemark P. O. J., (1996), Wet tropospheric effects on precise relative GPS height determination, Journal of Geodesy, 70, 188-202.

Heinkelmann R., Boehm J., Schuh H., Bolotin S., Engelhardt G., MacMillan D. S., Negusini M., Shurikhina E., Tesmer V., and Titov O., (2007), Combination of long time-series of tropospheric zenith delays observed by VLBI, Journal of Geodesy, 81, 483-501. Doi: 10.1007/s00190-007-0147z.

Huang N. E., Shen Z., Long S. R., Wu M. C., Shih H. H., Zheng Q., Yen N. –C., Tung C. C., and Liu H. H., (1998), The empirical mode decomposition and the Hilbert spectrum for nonlinear and non-stationary time series analysis. Proc. Roy. Soc. Lond., 454(903-993).

Huang N. E., and Attoh-Okine N. O., (2005), The Hilbert-Huang transform in engineering,Taylor & Francis.

Krügel M., Thaller D., Tesmer V., Rothacher M., Angermann D., and Schmid R., (2007), Tropospheric parameters: combination studies based on homogeneous VLBI and GPS data, Journal of Geodesy, 81, 515-527, doi: 10.1007/s00190-006-0127-8.

Mendes V. B., and Langley R. B., (1998), Optimization of tropospheric delay mapping function performance for height-precision geodetic applications, Proceedings of DORIS, 27-29 April, Toulouse, France.

Mendez P. J. C., Heinkelmann R., Boehm J., Weber R., and Schuh H., (2006), Contributions of GPS and VLBI for understanding station motions, Journal of Geodynamics, 41(1-3), 87-93, doi: 10.1016/j.

Pegram G. G. S., Peel M. C., and McMahon T. A., (2008), Empirical mode decomposition using rational splines: an application to rainfall time series, Proc. R. Soc. A., 464(1483-1501), doi: 10.1098/rspa.2007.0311.

Petrov L., and Boy J. –P., (2004), Study of atmospheric pressure loading signal in VLBI observations, Journal of geophysical research,109(B03405), doi: 10.1029/2003JB002500.

Radić V., Pasarić Z., and Šinik N., (2004), Analysis of Zagreb climatological data using empirically decomposed intrinsic mode functions, Geofizika, 21, 15-36.

Salisbury J. I., and Wimbush M., (2002), Using modern time series analysis techniques to predict ENSO events from the SOI time series. Nonlinear processes in Geophysics, 9, 341-345.

Shen S. P., Shu T., Huang N. E., Wu Z., North G. R., Carl T. R., and Easterling T. R., (2005), HHT analysis of the nonlinear and non-stationary annual cycle of daily surface air temperature data, in Hibert-Huang Transform: Introduction and Application, pp. 187– 210, ed. N. E. Huang and S. S. P. Shen (World scientific, Singapore), pp. 311.

Tregoning P., and van Dam T., 2005, Atmospheric pressure loading corrections applied to GPS data at the observation level, Geophysical Research Letters, 32, L22310, doi:10.1029/2005GL024104.

Van Dam T. M., and Herring T. A., (1994), Detection of atmospheric pressure loading using very long baseline interferometry measurements. Journal of geophysical research, 99(B3), 4505-4518.

Wang, C.-S., Liou, Y. –A., and Yeh T. –K., (2008), Impact of surface meteorological measurements on GPS height determination, Geophysical Research Letters, 35, L23809, doi:10.1029/2008GL035929.

Yin H., Huang D., and Xiong Y., (2008), Regional tropospheric delay modelling based on GPS reference station network, International association of geodesy symposia, 132, 185-188, doi: 10.1007/978-3-540-74584-6.

Zhaohua W., and Huang N. E., (2009). Ensemble empirical mode decomposition: a noise-assisted data analysis method, Advances in Data Adaptive Analysis, vol. 1, no. 1, pp. 1-41.